Progress In Electromagnetics Research, Vol. 141, 99–116, 2013

DIRECTION FINDING FOR BISTATIC MIMO RADAR USING EM MAXIMUM LIKELIHOOD ALGORITHM

Hao Wen Chen*, **Degui Yang, Hong Qiang Wang, Xiang Li, and Zhao Wen Zhuang**

College of Electronics Science and Engineering, National University of Defense Technology, Changsha 410073, P. R. China

Abstract—In this paper, we investigate an expectation-maximization (EM) maximum likelihood (ML) algorithm of direction finding (DF) for bistatic multiple-input multiple-output (MIMO) radar, where it is shown that the DF problem can be described as a special case of ML estimation with incomplete data. First, we introduce the signal and the noise models, and derive the ML estimations of the direction parameters. Considering the computational complexity, we make use of the EM algorithm to compute the ML algorithm, referred to EM ML algorithm, which can be applied to the arbitrary antenna geometry and realize the auto-pairing between direction-of-departures (DODs) and direction-of-arrivals (DOAs). Then the initialization is considered. In addition, both the convergence and the Cramer-Rao bound (CRB) analysis are derived. Finally, simulation results demonstrate the potential and asymptotic efficiency of this approach for MIMO radar systems.

1. INTRODUCTION

MIMO radar has gotten considerable attention in a novel class of radar system in the last decade ([1, 2] and references therein). There are two basic regimes of architecture considered in the current literature [3]. One is called statistical MIMO radar with widely separated antennas, which captures the spatial diversity of the target's radar cross section (RCS) [2]. The other is called coherent MIMO radar with colocated antennas, which can obtain the waveform diversity and larger degrees of freedom (DOF) to improve the target parameter estimation,

Received 1 May 2013, Accepted 22 June 2013, Scheduled 12 July 2013

* Corresponding author: Hao Wen Chen (chenhw@nudt.edu.cn).

parameter identifiability and more flexibility for transmit beampattern design [1]. Furthermore, based on the placement geometry of transmit and receive antennas, the coherent MIMO radar can be distributed into two classes: One is bistatic MIMO radar; the other is monostatic MIMO radar. In this paper, we mainly discuss a bistatic MIMO radar architecture, whose direction finding (DF) is considered extensively [4–8]. Furthermore, the corresponding results derived here can be extended to monostatic MIMO radar [9–11] stemming from its virtual array.

Target direction estimation is a basic function of a radar system [12–19]. Many advanced DF algorithms for MIMO radar have been extensively discussed in the current literature [4–11]. For example, the direction estimation proposed in [20] achieves more accurate results by extracting and making use of the phase delay information between each transmit/receive antenna pair. A joint direction of DOD and DOA estimation for bistatic MIMO radar via both estimation of signal parameters by the rotational invariance techniques (ESPRIT) and singular value decomposition (SVD) of cross-correlation matrix of the received data from two transmit subarrays is presented in [4], and the authors in [8] have presented a joint DOA and DOD estimation algorithm for bistatic MIMO radar via ESPRIT by means of the rotational factor produced by multi-transmitter. The polynomial root finding algorithm for the joint DOA-DOD estimation is given in [5]. Multitarget identification and localization using bistatic MIMO radar systems have been proposed in [30]. The authors in [9] have developed a new tri-iterative least-square (TI-LS) method for bearing estimation in MIMO radar.

However, among all estimation methods, maximum likelihood (ML) method has the best asymptotic performance and is, in some sense, robust against small sample numbers and coherent source signals [23]. Unfortunately, the high-dimensional search associated with the standard computation of ML is its handicap in applications. At all times, more works in dealing with the ML techniques have been devoted to decomposing the high-dimensional search problem into a sequence of much smaller dimensional search problems, which can drastically reduce their computational complexity and can handle the array of arbitrary geometry [31–34]. One of the popular approaches is the expectation-maximization (EM) algorithm [22], which is a well-known iterative method for finding the maximum likelihood estimate when the likelihood function is difficult to maximize directly. The EM algorithm has been applied to DF problem of passive array for a deterministic signal model [33] or for both deterministic and stochastic signal models [35], assuming known noise covariance.

In this paper, we propose an EM ML algorithm of direction finding for bistatic MIMO radar, which can be applied to the arbitrary antenna geometry and realize the auto-pairing between DODs and DOAs. For the statistical characteristic of noise, we assume that it is Gaussian with an unknown level, which is different from the most assumptions in [4–11], while more reasonable. Then, we apply the standard EM algorithm to bistatic MIMO radar. Since the EM algorithm is sensitive to initialization, the algorithm is initialized using the methods proposed in primary works [22–35]. The convergence of the EM ML algorithm is proven, and the rate of convergence is investigated. Considering evaluating the EM ML algorithm, we derive the Cramer-Rao bound (CRB) on the direction parameters. To simplify the computation, we use the concentrated CRB theory in [29], which can discard the nuisance parameters and only considers the interested ones, to calculate the CRB on the direction parameters.

This paper is arranged as follows. In Section 2, we show the general signal model for bistatic MIMO radar and its assumption first. Then, the ML estimations of direction parameters are derived. In Section 3, we first derive the EM ML algorithm for bistatic MIMO and give the suggestion of the initialization. The convergence and the CRB analyses are also derived. In Section 4, several simulation results are presented. Finally, Section 5 concludes the paper.

Notation: in this paper, we use boldface lowercase letters for vectors and boldface uppercase letters for matrices. Superscripts $\{\cdot\}^T$, $\{\cdot\}^{-1}$ and $\{\cdot\}^H$ for the transpose, inverse and complex conjugate transpose operator of a matrix, respectively. $\text{vec}\{\cdot\}$ denotes the vectorization operator (stacking the columns on top of each other) of a matrix. $\Re\{\cdot\}$ denotes the real part of a complex-value matrix. $\|\cdot\|$ denotes the Euclidean norm of a vector, and $\mathbf{I}_M$ and $\mathbf{1}_M$ are the Mth-order identity matrix, the column vector with M unity-elements, respectively. $\otimes$ and $\odot$ stand for Kronecker product and element wise product, respectively. Finally, $\nabla_{\mathbf{x}}$ represents the first-order partial derivative operator, i.e., $\nabla_{\mathbf{x}} = [\frac{\partial}{\partial x_1}, \ldots, \frac{\partial}{\partial x_N}]^T$.

2. PROBLEM STATEMENT

In this section, we will present the signal and the noise models used in this paper as well as the underlying assumptions needed for their validity first. Then, the maximum likelihood estimations of the target's directions are derived.

2.1. Data Model

Consider a bistatic MIMO radar system with M_t transmit antennas and M_r receive antennas, which are all identical and omnidirectional. For simplicity, assume all antennas and targets are on the same plane. The transmit and the receive antennas are located at $\mathbf{t}_i = [x_i^t, y_i^t]^T$, $i = 1, \ldots, M_t$ and $\mathbf{r}_l = [x_l^r, y_l^r]^T$, $l = 1, \ldots, M_r$, respectively, both in half-wavelength units. The results, obtained in this paper, can be extended to 3-dimensional (3-D) case easily. Assume that the transmit antennas simultaneously emit M_t temporally orthogonal waveforms, i.e., $\mathbf{x}[n] = [x_1[n], \ldots, x_{M_t}[n]]^T$, $n = 1, \ldots, N$, where N is the number of samples in one observation interval, then, $1/N \sum_{n=1}^{N} \mathbf{x}[n]\mathbf{x}^H[n] = \mathbf{I}_{M_t}$. There are K far-field targets within the same range bin located at (ϕ_k, φ_k), $k = 1, \ldots, K$, where ϕ_k and φ_k are the DOD and the DOA of the kth target, respectively. The data received by such an MIMO radar can be written as

$$\mathbf{y}[n] = \sum_{k=1}^{K} \mathbf{b}\left(\phi_k\right) \zeta_k \mathbf{a}^T\left(\varphi_k\right) \mathbf{x}[n] + \mathbf{e}[n], \quad n = 1, \ldots, N \tag{1}$$

where $\mathbf{y}[n] = [y_1[n], \ldots, y_{M_r}[n]]^T \in \mathbb{C}^{M_r \times 1}$ is the received data vector; $\mathbf{a}(\phi_k) = [e^{-j\mathbf{t}_1^T \mathbf{k}_k^t}, \ldots, e^{-j\mathbf{t}_{M_t}^T \mathbf{k}_k^t}]^T \in \mathbb{C}^{M_t \times 1}$ and $\mathbf{b}(\varphi_k) = [e^{-j\mathbf{r}_1^T \mathbf{k}_k^r}, \ldots, e^{-j\mathbf{r}_{M_r}^T \mathbf{k}_k^r}]^T \in \mathbb{C}^{M_r \times 1}$ are the steering vectors for the transmitting and receiving arrays of the kth target, respectively, where $\mathbf{k}_k^t = \pi[\cos\phi_k, \sin\phi_k]^T$ and $\mathbf{k}_k^r = \pi[\cos\varphi_k, \sin\varphi_k]^T$ are the wavenumber vectors; $\{\zeta_k \in \mathbb{C}\}_{k=1}^K$ are the target amplitudes, which are proportional to the radar-cross-section (RCS) of the targets; $\mathbf{e}[n]$ is the noise vector, here we only consider thermal noise component, which can be assumed that $\mathbf{e}[n]$ are independent and identically distributed circularly symmetric complex Gaussian random vectors with mean zero and an unknown covariance matrix $\mathbf{Q} = \sigma^2 \mathbf{I}_{M_r}$.

According to (1), the unknown parameters, to be estimated from the data vectors $\{\mathbf{y}[n]\}_{n=1}^N$, are $\zeta = [\zeta_\mathbf{1}, \ldots, \zeta_\mathbf{K}]^\mathbf{T}$, directional parameters $\boldsymbol{\nabla} = [\phi_1, \ldots, \phi_K]^T$ and $\boldsymbol{\varphi} = [\varphi_1, \ldots, \varphi_K]^T$ and noise covariance level σ^2, where the directional parameters $\boldsymbol{\phi}$ and $\boldsymbol{\varphi}$ are the ones of interest, while ζ and σ^2 are the unknown nuisance parameters.

2.2. DF with Maximum Likelihood Estimation

From [20, 21], the independent sufficient vector can be obtained as

$$\tilde{\boldsymbol{\eta}} \triangleq \mathrm{vec}\left(\frac{1}{\sqrt{N}} \sum_{n=1}^{N} \mathbf{y}[n]\mathbf{x}^H[n]\right) \approx \sum_{k=1}^{K} \zeta_k \mathbf{d}\left(\phi_k, \varphi_k\right) + \mathbf{v} \tag{2}$$

where

$$\mathbf{d}(\phi_k, \varphi_k) = \sqrt{N}\mathrm{vec}\left(\mathbf{b}(\phi_k)\,\mathbf{a}(\varphi_k)^T\right) \quad (3)$$

$$\mathbf{v} = \mathrm{vec}\left(\frac{1}{\sqrt{N}}\sum_{n=1}^{N}\mathbf{e}[n]\mathbf{x}^H[n]\right) \sim \mathcal{CN}\left(\mathbf{0}, \sigma^2\mathbf{I}_{M_tM_r}\right) \quad (4)$$

where $\mathbf{d}(\phi_k, \varphi_k)$ is equivalent to the response of size M_tM_r array relative to the kth target. Essentially speaking, (2) is equal to the following expression

$$\bar{\mathbf{y}}[n] = \sum_{k=1}^{K}\zeta_k\left(\mathbf{b}(\phi_k)\otimes\mathbf{a}(\varphi_k)\right) + \bar{\mathbf{e}}[n], \quad n = 1, \ldots, N \quad (5)$$

where $\bar{\mathbf{e}}[n]$ has the same statistical characteristic with $\mathbf{e}[n]$. The likelihood function of $\bar{\mathbf{Y}} = [\bar{\mathbf{y}}[1], \ldots, \bar{\mathbf{y}}[N]]$ can be given by

$$\ln f\left(\bar{\mathbf{Y}}\left|\boldsymbol{\nabla}, \boldsymbol{\varphi}, \zeta, \sigma^2\right.\right) = -\sum_{n=1}^{N}\Bigg[M_rM_t\ln\pi + M_rM_t\ln\sigma^2 + \frac{1}{\sigma^2}\left(\bar{\mathbf{y}}[n]-\mathbf{h}(\boldsymbol{\phi}, \boldsymbol{\varphi}, \zeta)\right)^H\left(\bar{\mathbf{y}}[n]-\mathbf{h}(\boldsymbol{\phi}, \boldsymbol{\varphi}, \zeta)\right)\Bigg] \quad (6)$$

where

$$\mathbf{h}(\boldsymbol{\phi}, \boldsymbol{\varphi}, \zeta) = \sum_{k=1}^{K}\zeta_k\left(\mathbf{b}(\varphi_k)\otimes\mathbf{a}(\phi_k)\right) \quad (7)$$

Hence, the ML estimator of $\boldsymbol{\phi}$, $\boldsymbol{\varphi}$, $\boldsymbol{\zeta}$ and σ^2 in (6) is given by

$$\left(\hat{\boldsymbol{\phi}}, \hat{\boldsymbol{\varphi}}, \hat{\boldsymbol{\zeta}}, \hat{\sigma}^2\right)_{\mathrm{ML}} = \arg\max_{\boldsymbol{\phi}, \boldsymbol{\varphi}, \boldsymbol{\zeta}, \sigma^2}\ln f\left(\bar{\mathbf{Y}}\left|\boldsymbol{\phi}, \boldsymbol{\varphi}, \boldsymbol{\zeta}, \sigma^2\right.\right) \quad (8)$$

After optimization with respect to $\hat{\boldsymbol{\zeta}}$ and $\hat{\sigma}^2$, the ML estimator for $\boldsymbol{\phi}$ and $\boldsymbol{\varphi}$ is given by

$$\left(\hat{\boldsymbol{\phi}}, \hat{\boldsymbol{\varphi}}\right)_{\mathrm{ML}} = \arg\max_{\boldsymbol{\phi}, \boldsymbol{\varphi}}\ln f\left(\bar{\mathbf{Y}}\left|\boldsymbol{\phi}, \boldsymbol{\varphi}, \hat{\boldsymbol{\zeta}}, \hat{\sigma}^2\right.\right) \quad (9)$$

Obviously, to resolve the ML estimate problem, the searches with the high computational complexity are needed. Moreover, realizing the auto-pairing between the DODs and DOAs is also a key capability of the DF algorithm for bistatic MIMO radar. In Section 3, we will propose a DF method using EM algorithm, which can reduce greatly the complexity of ML estimate and has the auto-pairing.

3. EM ML ALGORITHM

The EM ML algorithm is a very effective method for locating modes of a likelihood function. The basic idea of EM algorithm is as follows [23]: Rather than performing a complicated maximization, one works with augmented data that can simplify the calculation and performs a series of simple maximizations. More specially, each iteration consists of two steps: 1) E-step (expectation step), which calculates the conditional expectation of the complete-data log-likelihood, and 2) M-step (maximization step), which maximizes the augmented data likelihood. The E and M-steps iterate repeatedly until the estimates converge. For a detailed review of this method, we encourage readers to refer to [24]. In this section, we propose an EM ML direction finding algorithm for bistatic MIMO radar first, then we give its initial condition, convergence analysis, computational complexity, and CRB results.

3.1. EM ML Direction Finding Algorithm

According to the superposition property of array outputs [25], we give the augmented data $\mathbf{z}[n] = [z_1[n], \ldots, z_K[n]]^T$, $n = 1, \ldots, N$ first. Decomposing the expression in (5) into the following components as

$$\mathbf{z}_k[n] = \zeta_k \left(\mathbf{b}\left(\varphi_k\right) \otimes \mathbf{a}\left(\phi_k\right)\right) + \mathbf{e}_k[n], \quad k = 1, \ldots, K \tag{10}$$

Stacking $\mathbf{z}_k[n]$ into a matrix yields

$$\mathbf{Z}[n] = \left[\mathbf{z}_1^T[n], \ldots, \mathbf{z}_K^T[n]\right]^T = \begin{bmatrix} \zeta_1\left(\mathbf{b}\left(\varphi_1\right) \otimes \mathbf{a}\left(\phi_1\right)\right) \\ \vdots \\ \zeta_K\left(\mathbf{b}\left(\varphi_K\right) \otimes \mathbf{a}\left(\phi_K\right)\right) \end{bmatrix} + \begin{bmatrix} \mathbf{e}_1[n] \\ \vdots \\ \mathbf{e}_K[n] \end{bmatrix} \tag{11}$$

where $\mathbf{e}_k[n]$, $(n = 1, \ldots, N;\ k = 1, \ldots, K)$ are the noise processes, which are independent, complex Gaussian distributed with zero mean and covariance matrices $\sigma_k^2\mathbf{I}$, $k = 1, \ldots, K$, with the constraint $\sum_{k=1}^{K} \sigma_k^2 = \sigma^2$, $0 < \sigma_k^2 < \sigma^2$. Generally, a convenience choice is $\sigma_k^2 = \sigma^2/K$. Denote the estimated parameter vector by $\boldsymbol{\vartheta} = [\boldsymbol{\vartheta}_1, \ldots, \boldsymbol{\vartheta}_k, \ldots, \boldsymbol{\vartheta}_K]$, where $\boldsymbol{\vartheta}_k = [\phi_k, \varphi_k, \zeta_k, \sigma_k^2]$. Then, the augmented data log-likelihood function can be written as

$$\begin{aligned} \ln f_{\mathbf{Z}}\left(\boldsymbol{\vartheta}\right) &= -\sum_{k=1}^{K}\sum_{n=1}^{N}\left[M_r \ln\pi + \ln\sigma_k^2 + \frac{1}{\sigma_k^2}\left(\mathbf{z}_k[n] - \mathbf{h}\left(\boldsymbol{\phi}, \boldsymbol{\varphi}, \zeta\right)\right)^H\right. \\ &\quad \left. \cdot \left(\mathbf{z}_k[n] - \mathbf{h}\left(\boldsymbol{\phi}, \boldsymbol{\varphi}, \zeta\right)\right)\right] = \sum_{k=1}^{K} \ln f_{\mathbf{z}_k}\left(\boldsymbol{\vartheta}_k\right) \end{aligned} \tag{12}$$

According to (12), $\ln f_{\mathbf{Z}}(\boldsymbol{\vartheta})$ can be decomposed into a series of $\ln f_{\mathbf{z}_k}(\boldsymbol{\vartheta}_k)$ for the independence of $\mathbf{e}_k[n]$, $k = 1, \ldots, K$. Since $\ln f_{\mathbf{z}_k}(\boldsymbol{\vartheta}_k)$ depends only on the parameter vector $\boldsymbol{\vartheta}_k$, optimizing $\ln f_{\mathbf{Z}}(\boldsymbol{\vartheta})$ can be obtained by maximizing each $\ln f_{\mathbf{z}_k}(\boldsymbol{\vartheta}_k)$. Therefore, the complicated multidimensional search over $\boldsymbol{\phi}$ and $\boldsymbol{\varphi}$ is now replaced by a series of one-dimensional (1-D) searches, which is similar with the computationally efficient angle ML estimation for signals with known waveforms in [26]. It is worth to note that the decoupled estimation in [26] is a natural result (which results from the signal model for uncorrelated narrowband plane waves and unknown amplitudes), while the decoupled estimation in (12) is an asymptotic result.

Given the estimate of the ith iteration of $\boldsymbol{\vartheta}$ except for the noise level, i.e., $\boldsymbol{\phi}^{[i]}$, $\boldsymbol{\varphi}^{[i]}$ and $\boldsymbol{\zeta}^{[i]}$. Then, the $(i+1)$th iteration of the EM ML algorithm is as follows.

- E-step
  Compute
$$Q\left(\boldsymbol{\vartheta}, \boldsymbol{\vartheta}^{[i]}\right) = E\left\{\ln f_{\mathbf{Z}}(\boldsymbol{\vartheta})\,|\mathbf{Y}, \boldsymbol{\vartheta}^{[i]}\right\} \tag{13}$$
  which is equivalent to calculate the following conditional expectations:
$$\begin{aligned}
\sigma^{2[i]} &= \frac{1}{M_r M_t N}\sum_{n=1}^{N}\left[\left(\bar{\mathbf{y}}[n] - \mathbf{h}\left(\boldsymbol{\phi}^{[i]}, \boldsymbol{\varphi}^{[i]}, \boldsymbol{\zeta}^{[i]}\right)\right)^H \right. \\
&\quad \left. \cdot\left(\bar{\mathbf{y}}[n] - \mathbf{h}\left(\boldsymbol{\phi}^{[i]}, \boldsymbol{\varphi}^{[i]}, \boldsymbol{\zeta}^{[i]}\right)\right)\right] \qquad (14)\\
\hat{\mathbf{z}}_k\left(n, \boldsymbol{\vartheta}_k^{[i]}\right) &= E\left\{\mathbf{z}_k[n]\,\middle|\bar{\mathbf{Y}}, \boldsymbol{\vartheta}^{[i]}\right\} = \zeta_k^{[i]}\left(\mathbf{b}\left(\varphi_k^{[i]}\right)\otimes\mathbf{a}\left(\phi_k^{[i]}\right)\right) \\
&\quad + \frac{\sigma_k^2}{\sigma^{2[i]}}\left(\bar{\mathbf{y}}[n] - \mathbf{h}\left(\boldsymbol{\phi}^{[i]}, \boldsymbol{\varphi}^{[i]}, \boldsymbol{\zeta}^{[i]}\right)\right) \qquad (15)\\
\hat{\mathbf{R}}_{\mathbf{z}_k}\left(\boldsymbol{\vartheta}_k^{[i]}\right) &= E\left\{\frac{1}{N}\sum_{n=1}^{N}\mathbf{z}_k[n]\mathbf{z}_k^H[n]|\bar{\mathbf{Y}}, \boldsymbol{\vartheta}^{[i]}\right\} \\
&= \frac{1}{N}\sum_{n=1}^{N}\hat{\mathbf{z}}_k\left(n, \boldsymbol{\vartheta}_k^{[i]}\right)\hat{\mathbf{z}}_k^H\left(n, \boldsymbol{\vartheta}_k^{[i]}\right) + \frac{(\sigma_k^2)^2}{\sigma^{2[i]}}\mathbf{I} \qquad (16)
\end{aligned}$$

- M-step
  Update $\boldsymbol{\phi}^{[i]}$, $\boldsymbol{\varphi}^{[i]}$ and $\boldsymbol{\zeta}^{[i]}$ by maximizing $Q(\boldsymbol{\vartheta}, \boldsymbol{\vartheta}^{[i]})$, which is equivalent to the following K groups of equations:
$$\phi_k^{[i+1]} = \arg\max_{\phi_k}\frac{\left(\mathbf{b}\left(\varphi_k^{[i]}\right)\otimes\mathbf{a}(\phi_k)\right)^H\hat{\mathbf{R}}_{\mathbf{z}_k}\left(\boldsymbol{\vartheta}_k^{[i]}\right)\left(\mathbf{b}\left(\varphi_k^{[i]}\right)\otimes\mathbf{a}(\phi_k)\right)}{\left\|\mathbf{b}\left(\varphi_k^{[i]}\right)\otimes\mathbf{a}(\phi_k)\right\|^2} \tag{17}$$

$$\varphi_k^{[i+1]} = \arg\max_{\varphi_k} \frac{\left(\mathbf{b}(\varphi_k)\otimes\mathbf{a}\left(\phi_k^{[i+1]}\right)\right)^H \hat{\mathbf{R}}_{\mathbf{z}_k}\left(\boldsymbol{\vartheta}_k^{[i]}\right)\left(\mathbf{b}(\varphi_k)\otimes\mathbf{a}\left(\phi_k^{[i+1]}\right)\right)}{\left\|\mathbf{b}\left(\varphi_k\right)\otimes\mathbf{a}\left(\phi_k^{[i+1]}\right)\right\|^2} \tag{18}$$

$$\zeta_k^{[i+1]} = \frac{\left(\mathbf{b}\left(\varphi_k^{[i+1]}\right)\otimes\mathbf{a}\left(\phi_k^{[i+1]}\right)\right)^H}{N\left\|\mathbf{b}\left(\varphi_k^{[i+1]}\right)\otimes\mathbf{a}\left(\phi_k^{[i+1]}\right)\right\|^2}\sum_{n=1}^{N}\hat{\mathbf{z}}_k\left(n,\boldsymbol{\vartheta}_k^{[i]}\right) \tag{19}$$

- Terminating criterion
  If
  $$\max_k \left\|\boldsymbol{\vartheta}_k^{[i+1]} - \boldsymbol{\vartheta}_k^{[i]}\right\| < \varepsilon \tag{20}$$
  where ε is a small constant (which determines the number of iteration times and the estimate accuracy), $\hat{\boldsymbol{\vartheta}} = \boldsymbol{\vartheta}^{[i]}$, otherwise, $i = i + 1$, go to E-step.

3.2. Initial Conditions

Initialization of the EM algorithm is very important in order to reduce the likelihood of convergence to local extrema in the likelihood function, which will be validated in simulation part. Here, we give a revelatory method that all initial estimates of direction parameters are first computed by using the subspace-type algorithms proposed in [4–8], then, an initialization cycle of EM algorithm is carried out to calculate the initial estimates of remaining parameters, i.e., $\boldsymbol{\zeta}$ and σ^2. Till now, the initialization of the EM algorithm has been finished, and the E-M-step iteration will be repeated until some convergence criterion is achieved.

3.3. Convergence Analysis

In this section, we investigate the convergence property of the algorithm proposed in Section 3, which is based on [22, 23, 27, 28]. Using a Taylor expansion, in a neighborhood of an interior point of parameter space, $\boldsymbol{\vartheta}^*$, the estimates $\boldsymbol{\vartheta}^{[i]}$ have the following approximate relationship for sufficiently large i

$$\boldsymbol{\vartheta}^{[i+1]} - \boldsymbol{\vartheta}^* = \mathbf{M}\left(\boldsymbol{\vartheta}^{[i]} - \boldsymbol{\vartheta}^*\right) \tag{21}$$

where $\mathbf{M}$ is defined as the rate matrix of the algorithm. It is worth to note that the convergence rate is determined by the spectral radius

$\rho(\mathbf{M})$. Definitely speaking, a larger $\rho(\mathbf{M})$ means a slower convergence speed. According to [22], the rate matrix of the EM algorithm is

$$\mathbf{M} = \mathbf{I} - \mathcal{I}_{EM}^{-1}\mathcal{I}_{obs} \tag{22}$$

where

$$\mathcal{I}_{EM} = E\left\{-\nabla_{\boldsymbol{\vartheta}}\nabla_{\boldsymbol{\vartheta}}^T \ln f_{\mathbf{Z}}(\boldsymbol{\vartheta})\,|\mathbf{Y}, \boldsymbol{\vartheta}\right\}\Big|_{\boldsymbol{\vartheta}=\boldsymbol{\vartheta}^*} \tag{23}$$

is the excepted augmented information matrix, and

$$\mathcal{I}_{obs} = -\nabla_{\boldsymbol{\vartheta}}\nabla_{\boldsymbol{\vartheta}}^T \ln f_{\mathbf{Y}}(\boldsymbol{\vartheta})\Big|_{\boldsymbol{\vartheta}=\boldsymbol{\vartheta}^*} \tag{24}$$

is the observed information matrix. Based on the characteristic of the likelihood function in [23], we can get

$$\mathcal{I}_{EM} > \mathcal{I}_{obs} \tag{25}$$

then,

$$\mathcal{I}_{EM}^{-1} < \mathcal{I}_{obs}^{-1} \tag{26}$$

Thus

$$0 < \rho(\mathbf{M}) = \rho\left(\mathbf{I} - \mathcal{I}_{EM}^{-1}\mathcal{I}_{obs}\right) < 1, \tag{27}$$

i.e., the EM algorithm in Section 3 converges in its parameter space. It is worth to note that, if the exact convergence speed of EM algorithm is needed, we should calculate $\mathcal{I}_{EM}$ and $\mathcal{I}_{obs}$ in (22) first, and compute the spectral radius of $\mathbf{M}$. For the limit of the space, we do not give the detailed derivation.

3.4. Computational Complexity

In this subsection, we will analyze the computational complexity of our proposed EM ML algorithm. The main computational cost of our method is in E-step and M-step. For each iteration, computing σ^2 in (15) takes a complexity of about $O(NM_tM_r)$; for each target, computing $\hat{\mathbf{R}}_{\mathbf{z}_k}$ and $\hat{\mathbf{R}}_{\mathbf{z}_k}$ in E-step take $O(M_tM_r)$ and $O(N(M_tM_r)^2)$, respectively; in M-step, for each target, both the complexity for computing ϕ_k and φ_k is $O((M_tM_r)^3)$, and the complexity for computing ζ_k is $O(N(M_tM_r)^2)$. Therefore, the complexity per iteration of our EM ML algorithm is $O(NM_tM_r + K(M_tM_r + 2N(M_tM_r)^2 + (M_tM_r)^3))$. Assume the algorithm converges within L steps, then the total computational complexity of our method is about $O(LNM_tM_r + LK(M_tM_r + 2N(M_tM_r)^2 + (M_tM_r)^3))$.

For the same scenario, the total computational complexity of the TI-LS method in [9] is $O(N(2(M_tM_r)^3 + K(M_tM_r)^2 + K^2(M_tM_r) + 3LK^3 + 8LK^2))$. The computational complexity of our algorithm subtracts from the one of the TI-LS method gives about $O((2N - LK)(M_tM_r)^3)$. Since the number of sampling is usually large, i.e., $(2N - LK) > 0$, our proposed algorithm is more efficient than the algorithm in [9].

3.5. CRB Results

For the sake of evaluating the asymptotic performance of the EM ML algorithm in simulation part, we derive the CRB of unknown parameters, i.e., $\boldsymbol{\zeta}$, $\boldsymbol{\phi}$, $\boldsymbol{\varphi}$ and σ^2, according to (2). First, we rewrite (2) as the matrix form

$$\tilde{\boldsymbol{\eta}} = \mathbf{A}\left(\boldsymbol{\phi}, \boldsymbol{\varphi}\right)\boldsymbol{\zeta} + \mathbf{v} \tag{28}$$

where

$$\mathbf{A}\left(\boldsymbol{\phi}, \boldsymbol{\varphi}\right) = \left[\operatorname{vec}\left(\mathbf{b}\left(\varphi_1\right)\mathbf{a}^T\left(\phi_1\right)\right), \ldots, \operatorname{vec}\left(\mathbf{b}\left(\varphi_K\right)\mathbf{a}^T\left(\phi_K\right)\right)\right] \tag{29}$$

In what follows, we omit the arguments $\boldsymbol{\phi}$ and $\boldsymbol{\varphi}$ of $\mathbf{A}\left(\boldsymbol{\phi}, \boldsymbol{\varphi}\right)$ for simplicity. According to the data model in (28), the directional parameters $\boldsymbol{\phi}$ and $\boldsymbol{\varphi}$ are the ones of interest, while $\boldsymbol{\zeta}$ and σ^2 are nuisance parameters. To simplify the analytical computation, we use the concentrated CRB expression in [29]. Based on the *Theorem 3.1* in [29], the expression of CRB on $\boldsymbol{\phi}$ and $\boldsymbol{\varphi}$ is given by

$$\operatorname{CRB}\left(\boldsymbol{\phi}, \boldsymbol{\varphi}\right) = \frac{\sigma^2}{2N}\left\{\Re\left[\left(U \otimes \mathbf{1}_{2K}\right) \odot \left(\mathbf{D}^H \boldsymbol{\Pi}_c \mathbf{D}\right)^T\right]\right\}^{-1} \tag{30}$$

where

$$U = P\left(\mathbf{A}^H\mathbf{A}P + \sigma^2\mathbf{I}\right)^{-1}\mathbf{A}^H\mathbf{A}P \tag{31}$$

$$P = \sum_{k=1}^{K}|\zeta_k|^2 \tag{32}$$

$$\boldsymbol{\Pi}_c = \mathbf{I}_{M_tM_r} - \mathbf{A}\left(\mathbf{A}^H\mathbf{A}\right)^{-1}\mathbf{A}^H \tag{33}$$

$$\mathbf{D} = \left[\mathbf{d}_1^{(1)}, \ldots, \mathbf{d}_K^{(1)}, \mathbf{d}_1^{(2)}, \ldots, \mathbf{d}_K^{(2)}\right] \tag{34}$$

$$\mathbf{d}_k^{(1)} = \frac{\partial[\mathbf{A}]_k}{\partial\phi_k} = \frac{\partial\left(\operatorname{vec}\left(\mathbf{b}\left(\varphi_k\right)\mathbf{a}^T\left(\phi_k\right)\right)\right)}{\partial\phi_k} \tag{35}$$

$$\mathbf{d}_k^{(2)} = \frac{\partial[\mathbf{A}]_k}{\partial\varphi_k} = \frac{\partial\left(\operatorname{vec}\left(\mathbf{b}\left(\varphi_k\right)\mathbf{a}^T\left(\phi_k\right)\right)\right)}{\partial\varphi_k} \tag{36}$$

According to (33), now we consider the term

$$\mathbf{D}^H\boldsymbol{\Pi}_c\mathbf{D} = \mathbf{D}^H\mathbf{D} - \mathbf{D}^H\mathbf{A}\left(\mathbf{A}^H\mathbf{A}\right)^{-1}\mathbf{A}^H\mathbf{D} \tag{37}$$

Without loss of generality, we choose the origin of our coordinate system to be the array centroid of the transmit array. It is then clear that

$$\mathbf{D}^H\mathbf{A} = \mathbf{0}_{2K\times K} \quad \text{and} \quad \mathbf{A}^H\mathbf{D} = \mathbf{0}_{K\times 2K} \tag{38}$$

It follows immediately from (38) that the second term of (37) is zero. Thus, (30) can be simplified to

$$\operatorname{CRB}\left(\boldsymbol{\phi}, \boldsymbol{\varphi}\right) = \frac{\sigma^2}{2N}\left\{\Re\left[\left(U \otimes \mathbf{1}_{2K}\right) \odot \left(\mathbf{D}^H\mathbf{D}\right)^T\right]\right\}^{-1} \tag{39}$$

4. NUMERICAL EXAMPLES

We present some numerical examples that illustrate the performance of EM ML algorithms proposed in this paper, compared with that of the TI-LS method in [9]. In all simulations, we performed 500 Monte Carlo trials. Each following curves correspond to the mean over 500 simulations. Assume a bistatic MIMO radar with 4 transmit antennas and 4 receive antennas, where the half-wavelength spacing is respectively used. Without loss of generality, we assume the carrier frequency is $f = 5\,\text{GHz}$ and the pulse repetition interval is $T = 1/5000\,\text{s}$. The pulse duration is $T_p = N \times 5 \times 10^{-8}\,\text{s}$, where $N = 100$ is the number of sampling. Each transmit node uses uncorrelated quadrature phase shift keying (QPSK) waveforms. Four following scenarios, for comparisons, are considered:

Scenario 1: Assume three target are located at $(21^\circ, 10^\circ)$, $(44^\circ, 15^\circ)$ and $(63^\circ, 45^\circ)$, respectively, with the equal target amplitudes, i.e., $\zeta_1 = \zeta_2 = \zeta_3 = 1 \times e^{j\frac{\pi}{4}}$. The signal-to-noise (SNR), which is defined by the ratio of signal power to single channel noise power $10 \log[\sum_{n=1}^{N} \|x_i[n]\|^2/\sigma^2]$, ranges from -10 to $10\,\text{dB}$ with the step $2\,\text{dB}$. The maximum number of iteration is set to be 100. The initialization conditions are $(18^\circ, 14^\circ)$, $(40^\circ, 13^\circ)$ and $(60^\circ, 40^\circ)$, respectively. The algorithm is terminated if (20) is satisfied with $\varepsilon = 10^{-2}$. For comparison, the simulated annealing (SA) algorithm [36] is applied to the same batch of data to find the global ML estimate.

Scenario 2: Aiming to consider the convergence rate with termination condition, the specifications of this scenario is the same with the scenario 1, except for $\varepsilon = 5 \times 10^{-2}$.

Scenario 3: Aiming to investigate the effects of the separation of the targets in space, we assume three target are located at $(21^\circ, 10^\circ)$, $(22^\circ, 42^\circ)$ and $(63^\circ, 41^\circ)$, respectively, and the initialization conditions are $(18^\circ, 14^\circ)$, $(20^\circ, 41^\circ)$ and $(60^\circ, 40^\circ)$, respectively. The other specifications of this scenario is the same with the scenario 1.

Scenario 4: Aiming to study the effects of the initialization, we arbitrarily assume that the initialization conditions are $(10^\circ, 10^\circ)$, $(10^\circ, 10^\circ)$ and $(10^\circ, 10^\circ)$, respectively, which indicates that there is no prior information about the targets' direction. The other specifications of this scenario is the same with the scenario 1.

Figure 1 shows the curves of the iteration number and the root mean square error (RMSE) versus for scenario 1, respectively. We find that the number of iterations decreases with the increasing of SNR and the EM ML algorithm proposed in this paper has a good asymptotic performance in the higher SNR (more than $-5\,\text{dB}$). It

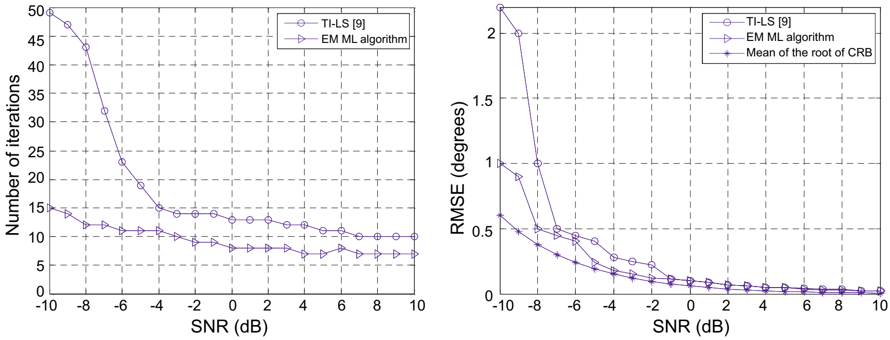

(a) (b)

Figure 1. Curves of iteration number and RMSE versus SNR for scenario 1. (a) Curve of iteration, (b) curve of RMSE.

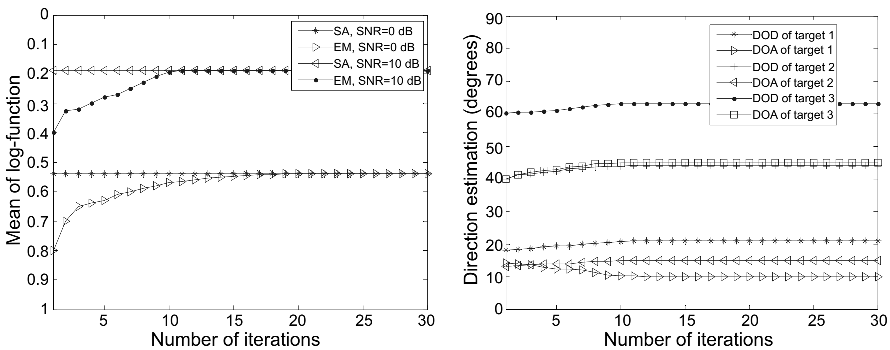

(a) (b)

Figure 2. Mean of log-function and direction estimations versus the number of iterations for scenario 1. (a) Curves of mean of log-function, (b) curves of direction estimations with SNR $=$ 10 dB. $[\hat{\boldsymbol{\phi}}, \hat{\boldsymbol{\varphi}}] = [20.8^\circ, 43.7^\circ, 62.9^\circ, 10.1^\circ, 15.2^\circ, 44.9^\circ]$.

is worth to note that the curves in Figure 1(b) are the arithmetical mean over the 500 trials. As expected, our EM ML algorithm is shown to be computationally more efficient and has a substantially better estimation performance than the TI-LS method. To examine the mean log-function of each iteration of EM ML algorithm, the mean log-function curve corresponding to the global ML estimate using SA algorithm is also portrayed in Figure 2(a) at SNR $= 0$, 10 dB. As expected, the log-likelihoods have a monotonic increase with iterations.

Furthermore, the EM ML algorithm attains the global maximum log-likelihood. Figure 2(b) depicts the direction estimates of each iteration at SNR = 10 dB. We can find that the direction parameters attains their true values after the larger number of iterations.

To examine the effects of termination condition on convergence rate, we show the mean of log-function and the direction estimates versus the number of iterations for scenario 2 in Figure 3, correspondingly to scenario 1 in Figure 2. According to Figure 3(a), the EM ML algorithm attains the global maximum log-likelihood more quickly than it in Figure 2(a), i.e., the scenario 2 has a faster convergence rate than scenario 1. However, the estimate accuracy is worse. Figure 2(b) shows that the iterates obtained by EM ML algorithm converge to $[\hat{\boldsymbol{\phi}}, \hat{\boldsymbol{\varphi}}] = [20.8°, 43.7°, 62.9°, 10.1°, 15.2°, 44.9°]$, whereas the Figure 3(b) shows that the iterates converge to $[\hat{\boldsymbol{\phi}}, \hat{\boldsymbol{\varphi}}] = [20.9°, 43°, 62.8°, 10.2°, 15.6°, 45.3°]$.

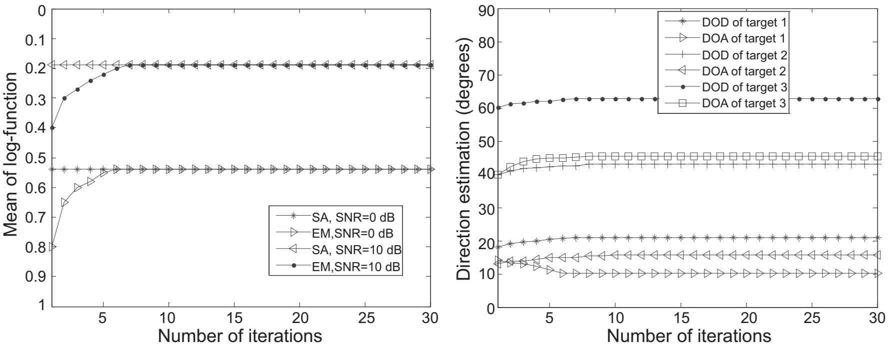

(a) (b)

Figure 3. Mean of log-function and direction estimations versus the number of iterations for scenario 2. (a) Curves of mean of log-function, (b) curves of direction estimations with SNR = 10 dB. $[\hat{\boldsymbol{\phi}}, \hat{\boldsymbol{\varphi}}] = [20.9°, 43°, 62.8°, 10.2°, 15.6°, 45.3°]$.

Figure 4 shows the curves of iteration number and RMSE versus SNR for scenario 3, respectively. Compared with Figure 1, we find that both EM ML algorithm and TI-LS method need more iteration times and attains a higher CRB with a higher RMSE. However, our EM ML algorithm is still shown to be computationally more efficient and has a substantially better estimation performance than the TI-LS method. This results from the effects of more adjacent targets, i.e., the more adjacent targets mean harder to estimate their direction

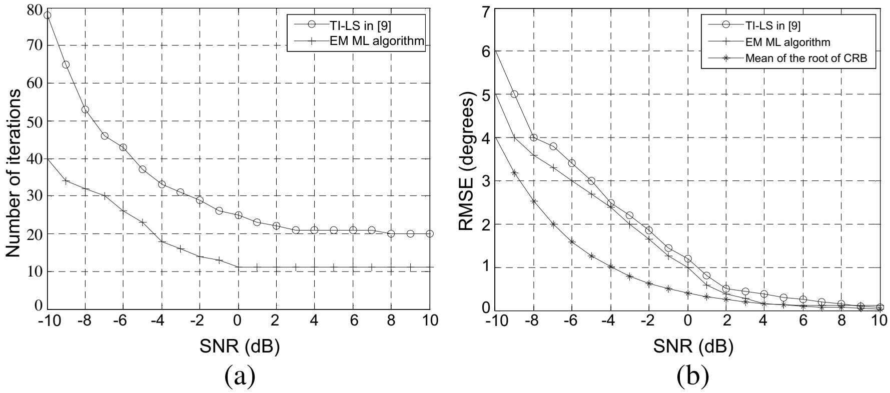

Figure 4. Curves of iteration number and RMSE versus SNR for scenario 3. (a) Curve of iteration, (b) curve of RMSE.

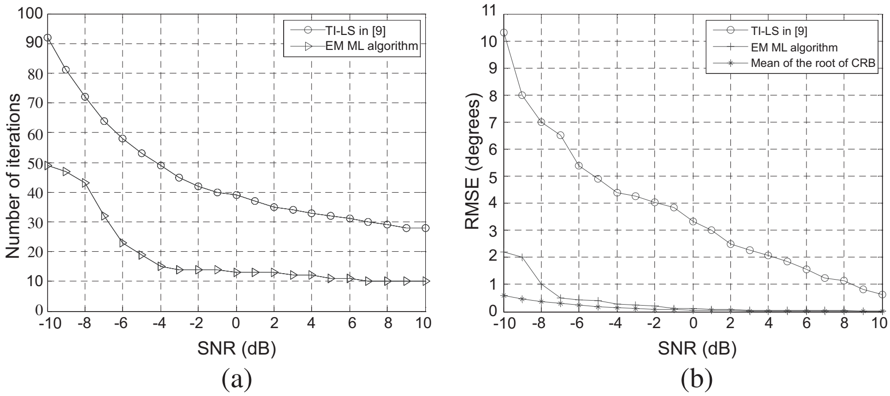

Figure 5. Curves of iteration number and RMSE versus SNR for scenario 4. (a) Curve of iteration, (b) curve of RMSE.

parameters [37]. Figure 5 shows the curves of iteration number and RMSE versus SNR for scenario 4, respectively. Similarly with Figure 4, we find that the EM ML algorithm needs more iteration times and attains the CRB with a higher RMSE, compared with Figure 1. Furthermore, both computational efficiency and estimation performance of EM ML algorithm are worse than TI-LS method. It demonstrates that the initialization conditions are very important for EM ML algorithm.

5. CONCLUSIONS

We have proposed an EM ML algorithm of DF for bistatic MIMO radar, which can be applied to the arbitrary antenna geometry and realize the auto-pairing between the DODs and the DOAs. First, we showed that the DF problem for bistatic MIMO radar can be described as a special case of ML estimation with incomplete data. Because of the high computational complexity associated with the standard implementation of ML, the EM algorithm, which decomposes the multi-dimensional search into a sequence of much smaller dimensional search problems, was used. Then, the methods of initialization, such as the subspace-type algorithms, were suggested. In addition, the convergence rate and the closed-form CRB expression of direction parameters were respectively derived. Finally, simulations demonstrate the potential of our estimates and confirm its asymptotic efficiency for MIMO radar systems. It is worth to note that the EM ML algorithm of DF for bistatic MIMO radar proposed in this paper can be extended to monostatic MIMO radar scenario correspondingly.

ACKNOWLEDGMENT

This work was supported by the Innovation Project for Excellent Postgraduates of the National University of Defense Technology and Hunan Province under No. B110402 and CX2011B018, respectively, P. R. China. The work of X. Li was supported in part by a grant from National Science Fund for Distinguished Young Scholars under No. 61025006. The author is very grateful for the insightful comments and suggestions made by the anonymous reviewers.

REFERENCES

1. Li, J. and P. Stoica, "MIMO radar with colocated antennas: Review of some recent work," *IEEE Signal Process. Mag.*, Vol. 24, No. 5, 106–114, Sep. 2007.
2. Haimovich, A. M., R. S. Blum, and L. Cimini, "MIMO radar with widely separated antennas," *IEEE Signal Process. Mag.*, Vol. 25, No. 1, 116–129, Jan. 2008.
3. Li, J. and P. Stoica, *MIMO Radar Signal Processing*, Wiley, New York, 2008.
4. Bencheikh, M. L., Y. D. Wang, and H. Y. He, "Polynomial root finding technique for joint DOA DOD estimation in bistatic MIMO radar," *Signal Processing*, Vol. 90, No. 9, 2723–2730, Sep. 2010.

5. Chen, J. L., H. Gu, and W. M. Su, "A new method for joint DOD and DOA estimation in bistatic MIMO radar," *Signal Processing*, Vol. 90, No. 2, 714–718, Feb. 2010.
6. Liu, X. L. and G. S. Liao, "Direction finding and mutual coupling estimation for bistatic MIMO radar," *Signal Processing*, Vol. 92, No. 2, 517–522, Feb. 2012.
7. Xie, R., Z. Liu, and J. X. Wu, "Direction finding with automatic pairing for bistatic MIMO radar," *Signal Processing*, Vol. 92, No. 1, 198–203, Jan. 2012.
8. Zheng, Z., J. Zhang, and J. Y. Zhang, "Joint DOD and DOA estimation of bistatic MIMO radar in the presence of unknown mutual coupling," *Signal Processing*, Vol. 92, No. 12, 3039–3048, 2012.
9. Lv, H., D. Z. Feng, H. W. Liu, J. He, and C. Xiang, "Tri-iterative least-square method for bearing estimation in MIMO radar," *Signal Processing*, Vol. 89, No. 12, 2686–2691, Dec. 2009.
10. Li, C. C., G. S. Liao, S. Q. Zhu, and S. Y. Wu, "An ESPRIT-like algorithm for coherent DOA estimation based on data matrix decomposition in MIMO radar," *Signal Processing*, Vol. 91, No. 8, 1803–1811, Aug. 2011.
11. Xie, R., Z. Liu, and Z. J. Zhang, "DOA estimation for monostatic MIMO radar using polynomial rooting," *Signal Processing*, Vol. 90, No. 12, 3284–3288, Dec. 2010.
12. Si, W., L. Wan, L. Liu, and Z. Tian, "Fast estimation of frequency and 2-D DOAs for cylindrical conformal array antenna using state-space and propagator method," *Progress In Electromagnetics Research*, Vol. 137, 51–71, 2013.
13. Cheng, S.-C. and K.-C. Lee, "Reducing the array size for DOA estimation by an antenna model switch technique," *Progress In Electromagnetics Research*, Vol. 131, 117–134, 2012.
14. Lie, J. P., B. P. Ng, and C. M. S. See, "Multiple UWB emitters DOA estimation employing time hopping spread spectrum," *Progress In Electromagnetics Research*, Vol. 78, 83–101, 2008.
15. Mukhopadhyay, M., B. K. Sarkar, and A. Chakraborty, "Augmentation of anti-jam GPS system using smart antenna with a simple DOA estimation algorithm," *Progress In Electromagnetics Research*, Vol. 67, 231–249, 2007.
16. Yang, P., F. Yang, and Z.-P. Nie, "DOA estimation with sub-array divided technique and interporlated ESPRIT algorithm on a cylindrical conformal array antenna," *Progress In Electromagnetics Research*, Vol. 103, 201–216, 2010.

17. Liang, J. and D. Liu, "Two L-shaped array-based 2-D DOAs estimation in the presence of mutual coupling," *Progress In Electromagnetics Research*, Vol. 112, 273–298, 2011.
18. Lizzi, L., F. Viani, M. Benedetti, P. Rocca, and A. Massa, "The M-DSO-ESPRIT method for maximum likelihood DOA estimation," *Progress In Electromagnetics Research*, Vol. 80, 477–497, 2008.
19. Agatonovic, M., Z. Stankovic, I. Milovanovic, N. Doncov, L. Sit, T. Zwick, and B. Milovanovic, "Efficient neural network approach for 2D DOA estimation based on antenna array measurements," *Progress In Electromagnetics Research*, Vol. 137, 741–758, 2013.
20. Bekkerman, I. and J. Tabrikian, "Target detection and localization using MIMO radars and sonars," *IEEE Trans. on Signal Process.*, Vol. 54, No. 10, 3873–3883, Oct. 2006.
21. Li, J., X. Xu, and P. Stoica, "Range compression and waveform optimization for MIMO radar: A Cramer-Rao bound based study," *IEEE Trans. on Signal Process.*, Vol. 56, No. 1, 218–232, Jan. 2008.
22. Dempster, A. P., N. M. Laird, and D. B. Rubin, "Maximum likelihood from incomplete data via the EM algorithm," *J. Roy. Statist. Soc. Ser. B*, Vol. 39, No. 1, 1–38, Jan. 1977.
23. Chung, P. J. and J. F. Bohme, "Comparative convergence analysis of EM and SAGE algorithms in DOA estimation," *IEEE Trans. on Signal Process.*, Vol. 49, No. 12, 2940–2949, Dec. 2001.
24. McLachlan, G. and T. Krishnan, *The EM Algorithm and Extensions*, John Wiley & Sons, New York, 1996.
25. Feder, M. and E. Weinstein, "Parameter estimation of superimposed signals using the EM algorithm," *IEEE Trans. on Acoust., Speech, Signal Process.*, Vol. 36, No. 4, 477–489, Apr. 1988.
26. Li, J., B. Halder, P. Stoica, and M. Viberg, "Computationally efficient angle estimation for signals with known waveforms," *IEEE Trans. on Signal Process.*, Vol. 43, No. 9, 2154–2163, Sep. 1995.
27. Wu, C. F. J., "On the convergence properties of the EM algorithm," *Ann. Statist.*, Vol. 11, No. 1, 95–103, Mar. 1983.
28. Hero, A. O. and J. A. Fessler, "Convergence in norm for alternating expectation-maximization (EM) type algorithms," *Statistica Sinica*, Vol. 5, No. 1, 41–54, Jan. 1995.
29. Hochwald, B. and A. Nehorai, "Concentrated Cramer-Rao bound expressions," *IEEE Trans. on Acoustics, Speech, and Signal Process.*, Vol. 40, No. 2, 363–371, Feb. 1994.

30. Yan, H. D., J. Li, and G. S. Liao, "Multitarget identification and localization using bistatic MIMO radar systems," *EURASIP J. Adv. Signal Process.*, Vol. 40, No. 1, 1–8, Jan. 2008.
31. Weiss, A. J., A. S. Willisky, and B. C. Levy, "Maximum likelihood array processing for estimation of superimposed signals," *Proc. IEEE*, Vol. 76, No. 2, 202–205, Feb. 1988.
32. Ziskind, I. and M. Wax, "Maximum likelihood localization of multiple suorces by alternating projection," *IEEE Trans. on Acoust., Speech, Signal Process.*, Vol. 36, No. 10, 1553–1560, Oct. 1988.
33. Feder, M. and E. Weistein, "Parameter estimation of superimposed signals using the EM algorithm," *IEEE Trans. on Acoust., Speech, Signal Process.*, Vol. 36, No. 4, 477–489, Apr. 1988.
34. Oh, S. K. and C. K. Un, "Simple computational methods of the AP algorithm for maximum likelihood localization of multiple radiating sources," *IEEE Trans. on Signal Process.*, Vol. 40, No. 11, 2848–2854, Nov. 1992.
35. Miller, M. I. and D. R. Fuhrmann, "Maximum-likelihood narrowband direction finding and the EM algorithm," *IEEE Trans. on Acoust., Speech, Signal Process.*, Vol. 38, No. 9, 1560–1577, Sep. 1990.
36. Kirkpatrick, S., C. D. Gelatt, and M. P. Vecchi, "Optimization by simulated annealing," *Science*, Vol. 220, No. 4598, 671–680, May 1983.
37. Chen, H. W., W. Zhou, J. Yang, Y. X. Peng, and X. Li, "Manifold studies on fundamental limits of direction finding MIMO radar systems," *IET Radar Sonar and Navigation*, Vol. 6, No. 8, 708–718, Dec. 2012.